

# Grain growth in Mn-doped ZnO

J. Han \*, P.Q. Mantas, A.M.R. Senos

*Department of Ceramic and Glass Engineering, University of Aveiro, 3810-193 Aveiro, Portugal*

## Abstract

Grain growth in ZnO doped with 0.1 to 1.2 mol% Mn was investigated during isothermal sintering from 1100 to 1300°C in air. Mn doping promotes the grain growth of ZnO during sintering, and this effect is enhanced by increasing the Mn doping level. The grain growth exponent is reduced from 3.4, for undoped ZnO, to 2.4, for ZnO doped with 1.2 mol% Mn, while the apparent activation energy for grain growth is reduced from 200 kJ/mol, for undoped ZnO, to 100–150 kJ/mol, for Mn-doped ZnO. Electrical measurements suggest that an excess of Mn probably exists at grain boundaries, either as a very thin second phase or as an amorphous film, which could benefit grain boundary diffusion, therefore promoting the grain growth of ZnO. © 2000 Elsevier Science Ltd. All rights reserved.

*Keywords:* Grain growth; Mn doping; Sintering; Varistors; ZnO

## 1. Introduction

ZnO based varistors exhibit highly nonlinear current–voltage characteristics and have been used extensively as electrical circuit protectors against power and voltage surges. A typical ZnO based varistor is a very complex chemical system and contains several dopants, such as Bi, Mn, Co, Sb, Al, and Cr. The effect of Mn doping on the electrical properties of ZnO varistor has been widely investigated, and it is generally accepted<sup>1–3</sup> that Mn doping can significantly improve the nonlinear current–voltage characteristics of ZnO varistors by affecting the defect chemistry at the grain boundaries.

The electrical properties of ZnO varistors are directly dependent on the composition and on microstructural characteristics, such as grain size, density, morphology and the distribution of second phases. The effect of some dopants, such as Al<sub>2</sub>O<sub>3</sub>,<sup>4–6</sup> Cr<sub>2</sub>O<sub>3</sub>,<sup>6</sup> Bi<sub>2</sub>O<sub>3</sub>,<sup>7</sup> Pr<sub>6</sub>O<sub>11</sub>,<sup>8</sup> and CuO,<sup>9</sup> on the sintering of ZnO have been investigated. The effect of Mn doping on the sintering of ZnO is important in order to understand the role of this element on ZnO varistor processing. In a previous work,<sup>10</sup> we studied the initial stage of sintering of Mn-doped ZnO under nonisothermal conditions, and concluded that the structure of ZnO grain boundaries was not affected by Mn doping from 0.1 to 1.2 mol% in the early stage of sintering.

In the present work, the effect of Mn doping on the grain growth of ZnO is investigated. This study was performed by isothermal sintering of ZnO doped with Mn in the range of 0.1–1.2 mol% from 1100 to 1300°C in air.

## 2. Experimental procedure

Reagent grade ZnO powder (Aldrich, Milwaukee, WI, USA) of 99.9% purity and a mean particle size of 0.26 μm was used. To dope with Mn, ethanol based solutions of hydrated manganese nitrate (Mn(NO<sub>3</sub>)<sub>2</sub>·4H<sub>2</sub>O) were prepared and mixed with ZnO powder in a planetary mill for 4 h. The amount of manganese ranged from 0.1 to 1.2 mol%. The slurry was dried, and the obtained powder was calcined at 450°C for 1 h, and isostatically pressed (200 MPa) as cylindrical pellets.

The temperature of a tube furnace was raised up to a predetermined value in the range of 1100–1300°C. Samples were quickly inserted into the center of the furnace. Appropriate corrections were made for the equilibration time so that the heat treatment of the individual samples may be considered isothermal. After sintering for a predetermined time in the range of 10–480 min, the samples were quenched to room temperature in air.

The relative densities of green and fired specimens were determined by the Hg-immersion method, using

\* Corresponding author.

5.65 g/cm<sup>3</sup> as the theoretical density of ZnO. X-ray diffractometry (XRD, Model Geigerflex, Rigaku Co., Tokyo, Japan) was used for phase analysis of the sintered specimens. The microstructures of the sintered specimens were observed by scanning electron microscopy (SEM, Hitachi S-4100), after polishing and thermal etching. The grain size was measured from SEM photomicrographs using the Quantimet 500+ Image Analysis System (Leica Cambridge Ltd, UK). The average grain size was obtained by the Schwartz-Saltykov method.<sup>11</sup> Grains 300–1000 were measured for each specimen to calculate the average grain size. Using a computer aided system, complex impedance of the samples was automatically measured with a Solartron 1260 Impedance Gain-Phase Analyser, in the frequency range of 1 Hz to 1 MHz.

### 3. Results and discussion

#### 3.1. Density and microstructure

Fig. 1 shows the relative density as a function of the sintering time for undoped and Mn-doped ZnO sintered at 1200°C. For all the compositions, the relative densities reach 94–96% after 10 min, and they are almost constant with further increases in sintering time. Therefore, the main densification process finished after 10 min sintering at 1200°C, behavior that was also observed in pure ZnO ceramics by Gupta and Coble.<sup>12</sup> No significant effect of Mn doping on the sintered density of ZnO was observed at this temperature. Fig. 2 presents the relative density of the sintered ceramic as a function of sintering temperature for undoped and Mn-doped ZnO sintered for 2 h. At each sintering temperature, the relative densities of ZnO doped with 0.1 and 0.3 mol% Mn are similar to that of undoped ZnO. However, when the Mn doping level is greater than 0.6 mol%, the rela-

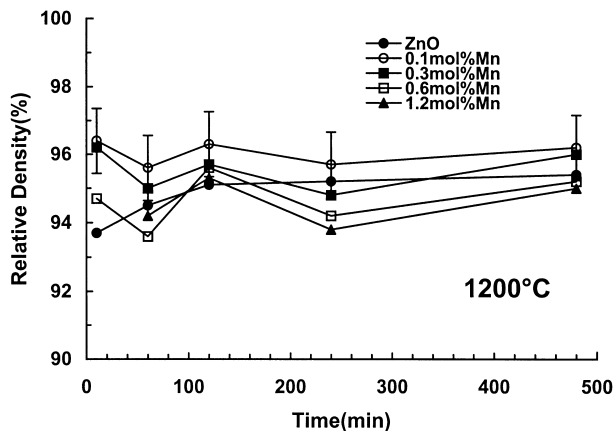


Fig. 1. Relative density as a function of sintering time for undoped and Mn-doped ZnO sintered at 1200°C. Since the errors of these densities are similar, only the error bars for 0.1% Mn are shown.

tive density increases with increasing the sintering temperature from 1100 to 1200°C, and then decreases with further increasing the temperature, and the relative densities at 1100 and 1300°C are lower than for undoped ZnO.

Fig. 3 shows the microstructures of undoped and Mn-doped ZnO sintered at 1200°C for 2 h. Similar microstructures were observed for undoped and Mn-doped ZnO at other sintering temperatures in this study. All the samples show uniform equiaxed grains and are free of abnormal grain growth. The grain growth of ZnO is promoted by Mn doping, but no significant change of the grain shape is observed. Although regular grain growth is observed for all the compositions, the grain size distribution broadens with the increase in Mn content. This effect is also observed in other doped ceramics systems<sup>13,14</sup> as a consequence of some heterogeneity in the additive distribution in the grain boundaries, which may result in different grain boundary mobilities due to the influence of the dopant on the grain boundary transport.

#### 3.2. Grain growth analysis

Fig. 4 illustrates the effect of sintering temperature on the grain growth of ZnO. The average grain size of each sample increases with increasing sintering temperature from 1100 to 1300°C. It is also observed that Mn doping promotes the grain growth of ZnO at each sintering temperature. Fig. 5 shows the average grain size as a function of the sintering time at 1200°C for Mn-doped ZnO with various Mn content. The relative densities of all the samples in Fig. 5 are similar between 94 and 96%, as shown in Fig. 1. Hence, the influence of densification on the grain growth is neglected. In Fig. 5, it is observed that, for ZnO doped with 0.1 mol% Mn, the average grain size is almost the same as for undoped ZnO, and that ZnO grain growth is promoted by Mn doping when the Mn content is greater than 0.3 mol%.

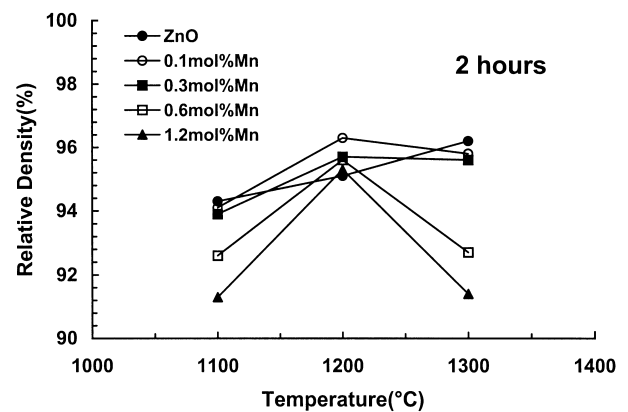


Fig. 2. Relative density as a function of sintering temperature for undoped and Mn-doped ZnO sintered for 2 h.

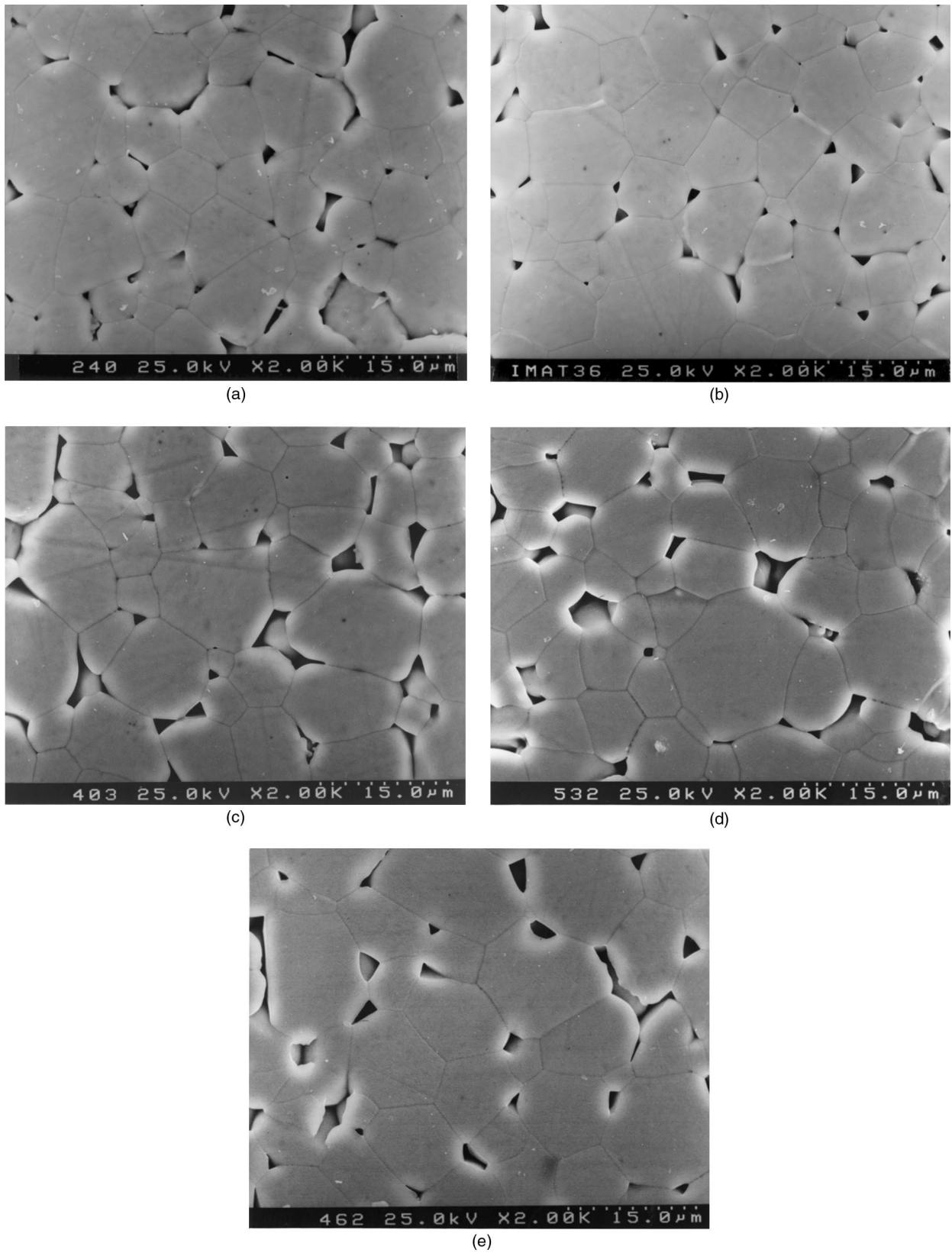


Fig. 3. Microstructures of undoped and Mn-doped ZnO sintered at 1200°C for 2 h: (a) undoped ZnO; (b) 0.1 mol% Mn; (c) 0.3 mol% Mn; (d) 0.6 mol% Mn; and (e) 1.2 mol% Mn.

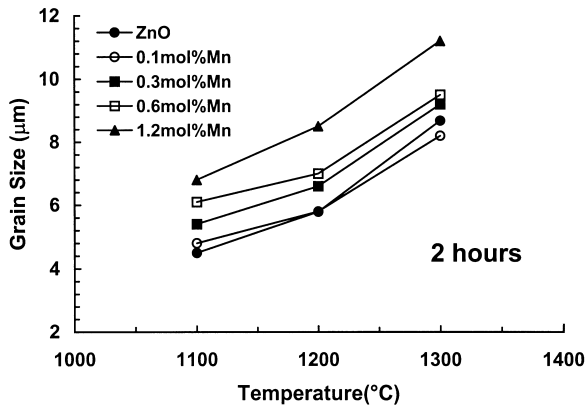


Fig. 4. Average grain size as a function of sintering temperature for undoped and Mn-doped ZnO sintered for 2 h.

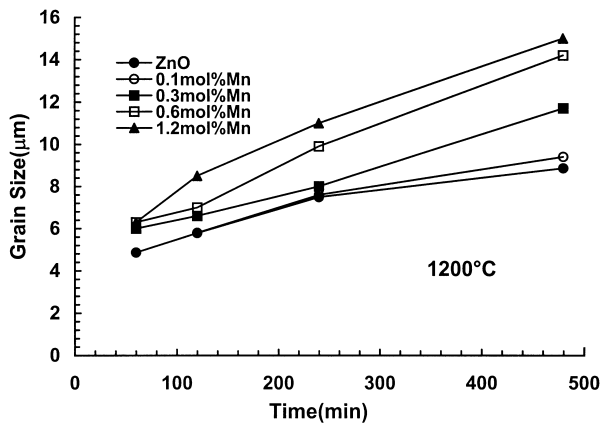


Fig. 5. Average grain size as a function of sintering time for undoped and Mn-doped ZnO sintered at 1200°C.

Grain growth kinetics can be described by the phenomenological kinetic grain growth equation:

$$G^n - G_0^n = K_0 t \exp(-Q/RT) \quad (1)$$

where  $G$  is the average grain size at the time  $t$ ,  $G_0$  is the initial grain size which is usually negligibly small,  $n$  is the kinetic grain growth exponent,  $K_0$  is a pre-exponential constant,  $Q$  is the apparent activation energy for the grain growth process,  $R$  is the gas constant, and  $T$  is the absolute temperature. According to Eq. (1), under isothermal conditions, the  $n$  value can be determined from the slope of the  $\log(G)$  versus  $\log(t)$  plot. The  $n$  values calculated from these plots in Fig. 6 are presented in Table 1. The grain growth exponent of undoped ZnO is close to 3, which has been observed for undoped ZnO by numerous researchers.<sup>7,12,15–17</sup> With increasing Mn doping level, the grain growth exponent is reduced from 3.4 for undoped ZnO to 2.4 for ZnO doped with 1.2 mol% Mn.

Fig. 7 shows the Arrhenius plots of  $\log(G^n/t)$  versus  $1/T$  for undoped and Mn-doped ZnO constructed from

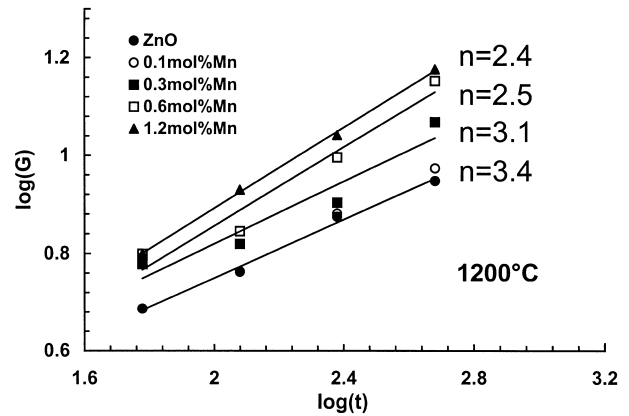


Fig. 6. Plots of  $\log(G)$  versus  $\log(t)$  for undoped and Mn-doped ZnO sintered at 1200°C.

Table 1

Grain growth exponent and apparent activation energy of undoped and Mn-doped ZnO

Composition	Grain growth exponent	Activation energy (kJ/mol)
Undoped ZnO	3.4	199
0.1% Mn-doped ZnO	3.4	162
0.3% Mn-doped ZnO	3.1	147
0.6% Mn-doped ZnO	2.5	100
1.2% Mn-doped ZnO	2.4	107

the data of Fig. 4. Eq. (1) can be expressed in the form ( $G_0$  being neglected)

$$\log(G^n/t) = \log(K_0) - 0.434(Q/RT) \quad (2)$$

the slope of which yields the apparent activation energy for the grain growth process. The activation energies obtained from the slopes of these Arrhenius plots in Fig. 7 are presented in Table 1. The activation energy for undoped ZnO obtained in this study is close to 200 kJ/mol, in good agreement with the results of numerous investigations of ZnO grain growth process.<sup>7,12,17,18</sup> Mn doping reduces the activation energy for grain growth of ZnO from 200 kJ/mol to 100–150 kJ/mol. This reduction of activation energy for ZnO grain growth in the presence of Mn also implies that Mn doping promotes the grain growth of ZnO.

The grain growth of several doped ZnO systems have been previously investigated. A similar reduction in the apparent activation energy for grain growth of ZnO is observed in the Bi-doped ZnO system ( $Q \sim 150$  kJ/mol)<sup>7</sup> in which grain growth is also promoted by the dopant, whereas the increase of the apparent activation energy and the retardation of ZnO grain growth are observed in the Sb-doped ZnO ( $Q \sim 600$  kJ/mol),<sup>19</sup>

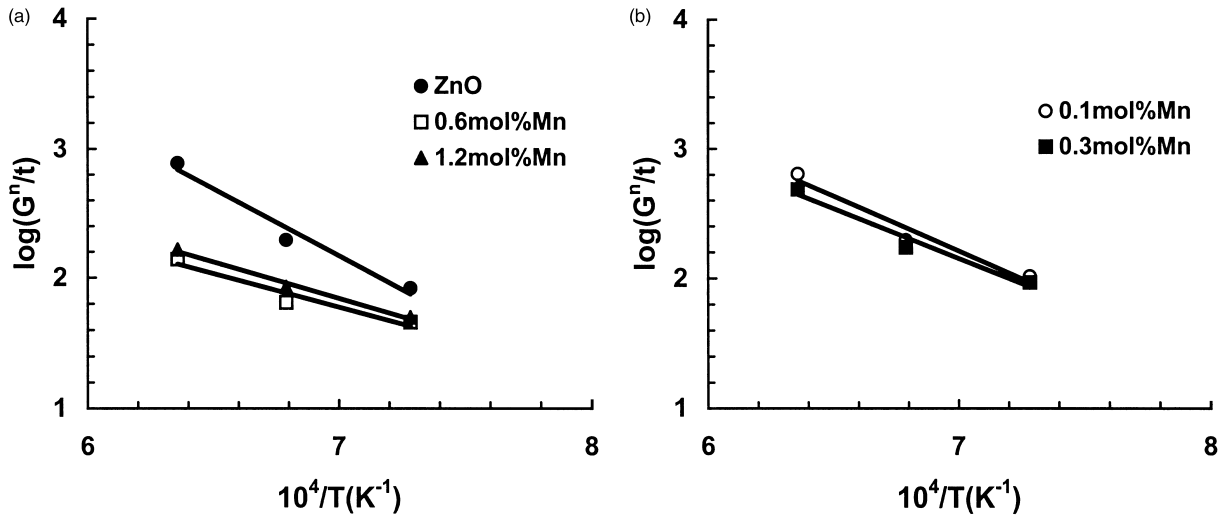


Fig. 7. Arrhenius plots of  $\log(G^n/t)$  versus  $1/T$  for undoped and Mn-doped ZnO: (a) undoped ZnO; 0.6 mol% Mn and 1.2 mol% Mn; (b) 0.1 mol% Mn and 0.3 mol% Mn.

K-doped ZnO ( $Q \sim 560$  kJ/mol),<sup>20</sup> Na-doped ZnO ( $Q \sim 310$  kJ/mol),<sup>21</sup> and Al-doped ZnO ( $Q \sim 400$  kJ/mol) systems.<sup>22</sup> From these observations, it was suggested that the dopants which promote the grain growth of ZnO form continuous grain boundary phases in ZnO ceramics. These continuous grain boundary phases could be liquid phases at sintering temperature, as observed in Bi-doped ZnO<sup>7</sup> and Ba-doped ZnO,<sup>23</sup> but may also be solid-state phases, as suggested for the Pr-doped ZnO<sup>8</sup> and Cu-doped ZnO<sup>9</sup> systems. By enhancing the mass diffusion transport at grain boundaries, these continuous grain boundary phases promote the grain growth of ZnO. From the results of XRD and SEM, no obvious second phase was observed for all the sintered samples in the present work. However, from complex impedance measurements, it was observed that, Mn doping induces a grain-boundary semicircle in the impedance spectra of ZnO doped with 0.3, 0.6 and

1.2 mol% Mn, while the impedance spectra of undoped ZnO and ZnO doped with 0.1 mol% Mn are devoid of any grain-boundary semicircle. Fig. 8 shows the impedance spectra with Cole–Cole representation for Mn-doped ZnO sintered at 1200°C for 8 h. The intercept of the grain-boundary semicircle with the real axis at the low-frequency end should be equal to  $R_{gb} + R_g$ , where  $R_{gb}$  is the grain-boundary resistance and  $R_g$  is the grain-bulk resistance, while the high-frequency end of the grain-boundary semicircle should intercept the real axis at  $R_{gi}$ . The resistivities of all the compositions constructed from Fig. 8 are presented at Table 2. It can be observed in Fig. 8 and Table 2 that Mn doping mainly increases the grain-boundary resistance with keeping the grain-bulk resistance almost unchanged. This suggests that excess Mn probably exists in the grain-boundary region, although no second phase is detected by XRD or SEM. Mn at the grain-boundary can exist as a very

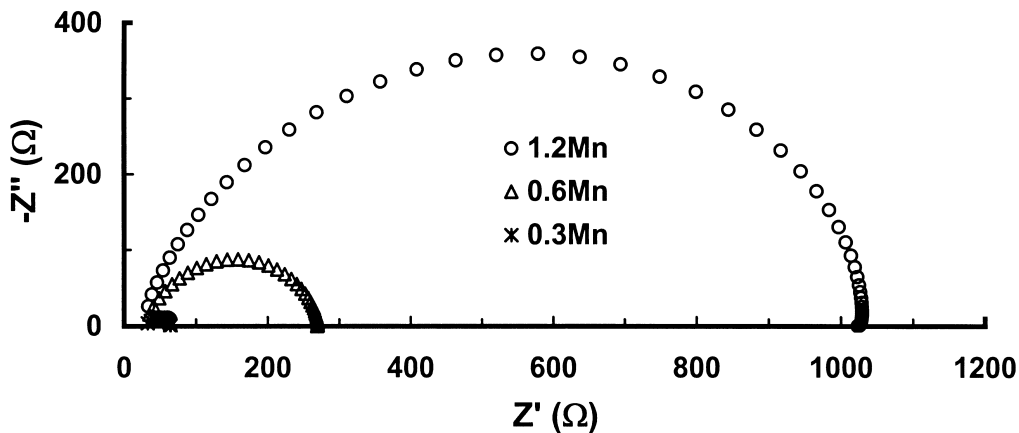


Fig. 8. Cole–Cole representation of the complex impedance, where  $Z'$  is the real part and  $Z''$  is the imaginary one, for Mn-doped ZnO sintered at 1200°C for 8 h.

Table 2

Relative density,  $D$ , average grain size,  $G$ , and resistivity,  $\rho$  of undoped and Mn-doped ZnO sintered at 1200°C for 8 h

Compositions	$D$ (%)	$G$ ( $\mu\text{m}$ )	$\rho$ ( $\Omega\text{cm}$ )
Undoped ZnO	95	8.9	10
0.1% Mn-doped ZnO	96	9.2	46
0.3% Mn-doped ZnO	96	11.7	228
0.6% Mn-doped ZnO	95	14.2	1050
1.2% Mn-doped ZnO	95	15.0	3128

thin second phase of the  $\text{ZnMnO}_3$  type in a nanometer scale, or as an amorphous Mn-rich film. The presence of a second phase or amorphous film can benefit grain boundary diffusion, thus promoting the grain growth of ZnO. Further careful microanalysis is necessary to evaluate the mechanism by which Mn affects the grain growth of ZnO. It is interesting to note that Bi, Ba, Pr, Cu, and Mn, which promote the grain growth of ZnO, also make ZnO ceramics show varistor behavior.

#### 4. Conclusion

Isothermal sintering of ZnO doped with Mn from 0.1 to 1.2 mol% was performed in the range of 1100 to 1300°C in air. The effect of Mn doping on the grain growth of ZnO was investigated. All the sintered samples in this study show uniform equiaxed grains and are free of abnormal grain growth. Mn doping promotes ZnO grain growth during sintering, and this promoting effect is enhanced with increasing Mn doping level. The grain growth exponent and the activation energy of undoped ZnO obtained in this study were found to be 3.4 and 200 kJ/mol, respectively, in good agreement with the results of other investigations on ZnO grain growth process. Mn doping reduces the grain growth exponent to a value of 2.4, for ZnO doped with 1.2 mol% Mn, and also reduces the activation energy to 100–150 kJ/mol. From complex impedance measurements, it was observed that Mn doping mainly increases the grain-boundary resistance with keeping the grain-bulk resistance almost unchanged. This fact suggests that excess Mn probably exists in the GB region, either as a very thin second phase or as an amorphous film, which could benefit the grain boundary transport for grain growth.

#### Acknowledgements

The author, Jiaping Han, would like to thank the financial support of the Praxis XXI programme of the Foundation for Science and Technology (FCT), Portugal

#### References

1. Einzinger, R., Metal oxide varistor action — a homojunction breakdown mechanism. *Appl. Surf. Sci.*, 1979, **1**, 329–340.
2. Tuller, M. H. and Boak, K.-K., Electrical activity at individual grain boundaries and interfaces in semiconducting oxides. In *Ceramic Transactions, Grain Boundaries and Interfacial Phenomena in Electronic Ceramics*, vol. 41, ed. L. M. Levinson. American Ceramic Society, Westerville, OH, 1994, pp. 19–34.
3. Greuter, F. and Blatter, G., Electrical properties of grain boundaries in polycrystalline compound semiconductors. *Semicond. Sci. Technol.*, 1990, **5**, 111–137.
4. Senos, A. M. R., Santos, M. R., Moreira, A. P. and Vieira, J. M., Grain boundary phenomena in the early stages of sintering of MO oxides. In *Surfaces and Interfaces of Ceramic Materials*, ed. L. C. Dufour, C. Monty and G. Petot-Ervas, NATO ASI Series. Kluwer Academic, London, 1989, pp. 553–556.
5. Senos, A. M. R., Vieira, J. M., Pore size distribution and particle rearrangement during sintering. In *Proceedings of the International Conference Third Euro-Ceramics* vol 1, ed. P. Duran and J. F. Fernandez. Faenza Editrice Iberica S. L., Faenza, 1993, pp. 821–826.
6. Senos, A. M. R., Sintering kinetics in open porosity stages of zinc oxide. PhD Thesis, University of Aveiro, Aveiro, 1993.
7. Senda, T. and Bradt, R. C., Grain growth in sintering ZnO and ZnO-Bi<sub>2</sub>O<sub>3</sub> ceramics. *J. Am. Ceram. Soc.*, 1990, **73**, 106–114.
8. Sida, M., Chun, S., Wakiya, N., Shinozaki, K. and Mizutani, N., Effect of the sintering temperature and atmosphere on the grain growth and grain boundary phase formation of Pr-doped ZnO varistor. *Yogyo Kyokaiishi*, 1996, **104**, 44–48.
9. Chiou, B. and Chung, M., Effect of copper additive on the microstructure and electrical properties of polycrystalline zinc oxide. *J. Am. Ceram. Soc.*, 1992, **75**, 3363–3368.
10. Han, J., Senos, A. M. R. and Mantas, P. Q., Nonisothermal sintering of Mn-doped ZnO. *J. Eur. Ceram. Soc.*, 1999, **19**, 1003–1006.
11. Dallavalle, J. M., Particle- and grain-size distributions. In *Quantitative Stereology*, ed. E. E. Underwood. Addison-Wesley, Reading, MA, 1971, pp. 109–147.
12. Gupta, T. K. and Coble, R. L., Sintering of ZnO: I, densification and grain growth. *J. Am. Ceram. Soc.*, 1968, **51**, 521–525.
13. Brook, R. J., Controlled grain growth. In *Treatise on Materials Science and Technology*, vol. 9, ed. F. F. Y. Wang. Academic Press, New York, 1976, pp. 331–364.
14. Kim, J., Kimura, T. and Yamaguchi, T., Microstructure development in Sb<sub>2</sub>O<sub>3</sub>-doped ZnO. *J. Mater. Sci.*, 1989, **24**, 2581–2586.
15. Nicholson, G. C., Grain growth in zinc oxide. *J. Am. Ceram. Soc.*, 1965, **48**, 214–215.
16. Quadir, T. and Readey, D. W., Microstructure development of zinc oxide in hydrogen. *J. Am. Ceram. Soc.*, 1989, **72**, 297–302.
17. Dutta, S. K. and Spriggs, R. M., Grain growth in fully dense ZnO. *J. Am. Ceram. Soc.*, 1970, **53**, 61–62.
18. Wong, J., Sintering and varistor characteristics of ZnO-Bi<sub>2</sub>O<sub>3</sub> ceramics. *J. Appl. Phys.*, 1980, **51**, 4453–4459.
19. Senda, T. and Bradt, R. C., Grain growth of zinc oxide during the sintering of zinc oxide-antimony oxide ceramics. *J. Am. Ceram. Soc.*, 1991, **74**, 1296–1302.
20. Gupta, T. K., Inhibition of grain growth in ZnO. *J. Am. Ceram. Soc.*, 1971, **54**, 413–414.
21. Watari, T. and Bradt, R. C., Grain growth of sintering ZnO with alkali oxide additions. *J. Ceram. Soc., Japan*, 1993, **101**, 1085–1089.
22. Nunes, S. I. and Bradt, R. C., Grain growth of ZnO and ZnO-Bi<sub>2</sub>O<sub>3</sub> ceramics with Al<sub>2</sub>O<sub>3</sub> additions. *J. Am. Ceram. Soc.*, 1995, **78**, 2469–2475.
23. Fan, J. and Freer, R., Varistor properties and microstructure of ZnO-BaO. *J. Mater. Sci.*, 1997, **32**, 415–419.